Vibrational relaxation in oxygen and nitrogen

By VERNON BLACKMAN†
Palmer Physical Laboratory, Princeton University

(*Received* 28 *December* 1955)

SUMMARY

A converging channel of area ratio 34 : 1 has been developed to produce strong shock waves in a tube. Shock waves of speeds $M_1 = 3$–$7{\cdot}5$ in oxygen and $M_1 = 5$–10 in nitrogen have now been studied with an interferometer, and values of the relaxation time τ for the approach to vibrational equilibrium behind the shocks have been measured. The value of τ (atmospheric) varies from 54 μsec at 800° K to 1·3 μsec at 3000° K for oxygen and from 19 μsec at 3500° K to 5 μsec at 5500° K for nitrogen. For oxygen, the graph of $\log\tau$ against $T^{-1/3}$ is not quite the straight line predicted by the Landau–Teller theory. The density ratios across the shocks were measured and compared with values calculated by the Bethe–Teller method for variable specific heats. Agreement between the measured and calculated values is satisfactory. Experiments were also performed on oxygen–nitrogen mixtures to determine the effect of nitrogen on the approach to equilibrium of the oxygen. It was found that O_2 and N_2 collisions at approximately 2000° K are 40% as effective in transferring energy to the oxygen as O_2 and O_2 collisions. A device that detects a shock with a time lag of less than 1 μsec, consisting of an evaporated gold film which changes its resistance when heated by the shock, was also developed.

INTRODUCTION

The purpose of this investigation was to determine the state variables for a strong shock wave whose Mach number, $M_1 = v_1/a_1$ (v_1 is the velocity of the incoming gas relative to the shock and a_1 is the velocity of sound in it), is so high that the approximation of constant specific heats is no longer applicable, and, where possible, to measure the relaxation times for the approach to equilibrium behind the shock.* Particular effort was made to study oxygen and nitrogen in the range $M_1 = 3$–10, and the results are compared with certain theoretical work concerning relaxation effects, and also with the relatively scarce experimental data for O_2 and N_2 that already exists.

* A fuller description of the work reported in this paper can be found in the author's doctoral dissertation, on file at the Princeton University library.

Owing to variation of the specific heats of oxygen and nitrogen for temperatures much above a few hundred degrees Kelvin, the Rankine–Hugoniot equations with constant specific heat ratio are not accurate for shock waves of Mach number 2 or greater. As the Mach number increases, this discrepancy also increases. For these stronger shock waves, the equilibrium static temperature behind the shock, T_2, is so high that the vibrational modes of a diatomic gas become excited, thus changing the specific heat of the gas. (This static temperature of the gas is a measure of the random molecular velocity, irrespective of the mass flow as a whole.) If the shock strength becomes great enough, and T_2 high enough, dissociation of the molecules can take place, and, for still higher temperatures, even ionization may occur. In the present investigation, however, only vibration effects are studied since T_2 was low enough for dissociation and ionization effects to be negligible. A method of calculating the shock wave properties, taking into account this variation of specific heat with temperature, has been developed by Bethe & Teller (1951).

The process by which a sudden increase in energy is distributed among the various degrees of freedom of a gas is very complex. Such a sudden increase in energy occurs when a shock wave passes through a gas. However, if the gas is diatomic, the redistribution of energy is not instantaneous. The translational degrees of freedom arrive at a Maxwellian distribution in the space of a few collisions. It can also be shown that the energy of rotation approaches equilibrium with energy of translation very rapidly, again within several collisions. This state is not the final equilibrium state of the gas, since, for molecules having vibrational states, the time necessary for the energy of vibration to come into equilibrium at the final temperature is known, in some cases, to be many thousand times that required for translation and rotation. This time, which is characteristic of the process, may be represented by a relaxation time for vibration, τ.

Pierce (1925), using the magnetostriction oscillator for determining sound velocities, was the first to measure sound dispersion. Herzfeld & Rice (1928) showed that dispersion could be explained by ascribing a time for readjustment of the vibrational energy which was long compared with the time for adjustment of translation and rotation. This led to the designation of translation and rotation as 'external' degrees of freedom, and modes such as vibration or ionization, which take a relatively long time to adjust themselves to external conditions, as 'internal' degrees of freedom. In the theory of sound dispersion the total specific heat C_p may be thought of as being made up of two parts:

$$C_p = C_p' + C_{\text{vib}}, \tag{1}$$

where C_p' is the specific heat due to the external degrees of freedom, and C_{vib} is the specific heat in vibration. Since the energy in the vibrations responds slowly to external changes, C_{vib} depends on the frequency of the sound. Thus, for very low frequencies, C_{vib} can follow the effects of the

compressions, but, for much higher frequencies, the time between compressions and rarefractions can become short compared with the adjustment time for vibration, and the effective specific heat of the gas does not include C_{vib}. This means that the effective value of γ for the gas increases, which in turn means that the velocity of sound also increases. At intermediate frequencies, the energy in vibration partially follows the changes in pressure but is out of phase with it. This causes the sound absorption to pass through a maximum. Thus, measurements of sound absorption as a function of frequency enable vibrational relaxation times to be determined. The method is well described by Herzfeld (1953).

A second method for measuring relaxation times was suggested by Kantrowitz (1942). In this method one allows a jet of gas to expand through a nozzle in a time which is long compared with the relaxation time, so that the full C_p of the gas is active. If this jet is then stopped at the head of a pitot tube in a time which is short compared with the relaxation time, only the specific heat of the external degrees of freedom is important. Then the difference between the tank pressure before the expansion and the stagnation pressure measured by the pitot tube is a measure of the energy lag in the gas. When the jet is stopped in a time of the order of τ, the relaxation time for this lag can be determined from the dimensions of the tube and the streamlines of the flow. Kantrowitz & Huber (1947) and Griffith (1950) have used this technique to determine the relaxation times for a number of gases, and the method seems well established.

A third method for determining relaxation times, which makes use of a shock tube and interferometer, was suggested in 1950 by Griffith. Measurements of τ for CO_2, N_2O, and methane have been made by this method at Princeton by Griffith, Brickl & Blackman (1956), and measurements on CO_2 and Cl_2 have been made by Smiley, Winkler & Slawsky (1954). The big advantage of this method over the two previous methods is that, by using various shock strengths, the value of τ for widely different temperatures can be determined. This serves to give a convenient check on a theory by Landau & Teller (1946) which predicts the dependence of τ on the temperature.

Theory

The Rankine–Hugoniot equations are exact expressions only for perfect gases with constant specific heat. Since the specific heat changes with temperature, it is clear that these equations are not accurate for strong shock waves. For argon, Resler, Lin & Kantrowitz (1950) have shown that this change in specific heat is slight up to $M_1 = 9$; however, above $M_1 = 9$ in argon, where temperatures greater than 8000° K are produced, ionization begins to occur and the specific heat may no longer be treated as a constant.

For diatomic gases such as oxygen or nitrogen the dependence of C_p on temperature is of importance at about 500° K, and for carbon dioxide this variation of C_p is of considerable significance even at room temperature. The translational and rotational modes of O_2 and N_2 are fully excited to the

classical value of $R/2$ per degree of freedom per mole at room temperature, while vibration and especially dissociation and ionization are excited to such a small extent that the energy in these modes may be neglected. As the temperature of the gas increases, these internal degrees of freedom can become excited, with the vibrational mode being the first excited since it has the lowest energy. For diatomic gases the energy in vibration, E_{vib}, is given by

$$E_{\text{vib}} = RT \frac{\theta/\text{T}}{\exp(\theta/\text{T}) - 1}, \tag{2}$$

where $\theta = h\nu/k$ is the characteristic temperature for vibration. For nitrogen $\theta = 3336°$ K, while for oxygen $\theta = 2228°$ K. For oxygen C_p increases, due to vibrations, by $1{\cdot}27R$ for an increase of temperature from 300° to 3000° K, while for the same increase of temperature in nitrogen C_p increases by $0{\cdot}95R$. In oxygen about 6% of the molecules are dissociated at 3500°K, and in nitrogen only about 1% are dissociated at 5000° K (according to Bethe & Teller 1951). Here, only the energy in vibration will be considered, since the change in C_p due to dissociation, even though appreciable at the strongest shocks obtained, is characterized by such a long relaxation time that these effects did not show up in the region behind the shock that could be observed.

In the Bethe–Teller method for calculating the shock parameters for the case of variable specific heat, one considers a one-dimensional shock wave moving through a gas. Then the conservation equations may be written:

mass, $$\rho_1 v_1 = \rho_2 v_2; \tag{3}$$

momentum, $$p_1 + \rho_1 v_1^2 = p_2 + \rho_2 v_2^2; \tag{4}$$

energy, $$E_1 + p_1/\rho_1 + v_1^2/2 = E_2 + p_2/\rho_2 + v_2^2/2. \tag{5}$$

For most gases at ordinary densities the perfect gas law applies:

$$p/\rho = RT. \tag{6}$$

These four equations uniquely determine the equilibrium values of the shock wave parameters, independently of the manner in which the equilibrium is attained.

From these equations, one is able to calculate the density, temperature, and pressure ratios as functions of M_1 for any strength of shock, provided the dependence of C_p on temperature is known. In order to facilitate these calculations, Bethe & Teller define a new quantity:

$$\beta_{(T)} = 1 + E_{(T)}/RT, \tag{7}$$

where $E_{(T)}$ is the total energy content per unit mass. If equilibrium exists, it can be shown that β is a function of temperature only. The energy equation can be rewritten in terms of β:

$$\beta_1 RT_1 + v_1^2/2 = \beta_2 RT_2 + v_2^2/2. \tag{8}$$

The solution of these equations can now be obtained. The density ratio across the shock is given by

$$\rho_2/\rho_1 = b + \sqrt{b^2 + T_1/T_2}, \tag{9}$$

where

$$b = \beta_2 - 1/2 - (\beta_1 - 1/2)T_1/T_2. \tag{10}$$

The Mach number is given by

$$M_1^2 = 2(\beta_2 T_2 - \beta_1 T_1)/\gamma_1 T_1[1 - (\rho_1/\rho_2)^2], \tag{11}$$

in which γ_1 is the ratio of the specific heats at the temperature T_1. For the calculations on oxygen and nitrogen, values for β were taken from the reports on these gases by Woolley (1953 a, b). It should be remembered that ρ_2 and T_2 refer to the final equilibrium values behind the shock wave. According to this viewpoint, the shock thickness includes the region that is necessary for vibrational equilibrium to be reached. This transition region may be very broad and depends on the pressure and temperature behind the shock.

Since the density and the speed of the shock are the two quantities that are measured directly by experiment, they are of the most importance as far as comparing theory with experiment is concerned. The pressure ratio across the shock may be obtained from the equation

$$p_2/p_1 = \rho_2 T_2/\rho_1 T_1. \tag{12}$$

Figure 1 shows the pressure, density, and temperature ratios across a shock of speed M_1 in oxygen, as calculated by the method outlined above. The same quantities, as found by the Rankine–Hugoniot relations with constant specific heat ratio, are plotted for comparison. Table 1 gives numerical values for the quantities used in the calculation, while table 2 gives the same quantities for N_2.

In figure 1, the curves for constant specific heat are labelled as ρ_a/ρ_1, etc. State a here represents the region immediately behind the shock which is characterized by equilibrium between translation and rotation but no change in the vibrational energy. For any gas, the variables at state a can be calculated from the Rankine–Hugoniot equations if the contribution of the vibrational energy to C_v is omitted. For oxygen and nitrogen, the Rankine–Hugoniot equations with $\gamma = 1{\cdot}40$ can be used to calculate variables in state a, since the amount of vibrational energy at room temperature is negligible.

The transition between state a and the final equilibrium is characterized by a changing energy of vibration, E_{vib}, for which Landau & Teller have derived the relaxation equation from general quantum considerations. They assume that the molecules are free to vibrate in any quantum level, but that changes in energy occur for $n = \pm 1$ only. If k_{10} and k_{01} are the probabilities of de-excitation and excitation per unit time respectively, between the ground and first excited states, then

$$k_{01} = k_{10} \exp(-h\nu/kT) \tag{13}$$

from the principle of detailed balancing. Likewise, for other quantum states,

$$k_{n,n-1} = nk_{10}\,, \tag{14}$$

and

$$k_{n-1,n} = k_{n,n-1} \exp(-h\nu/kT). \tag{15}$$

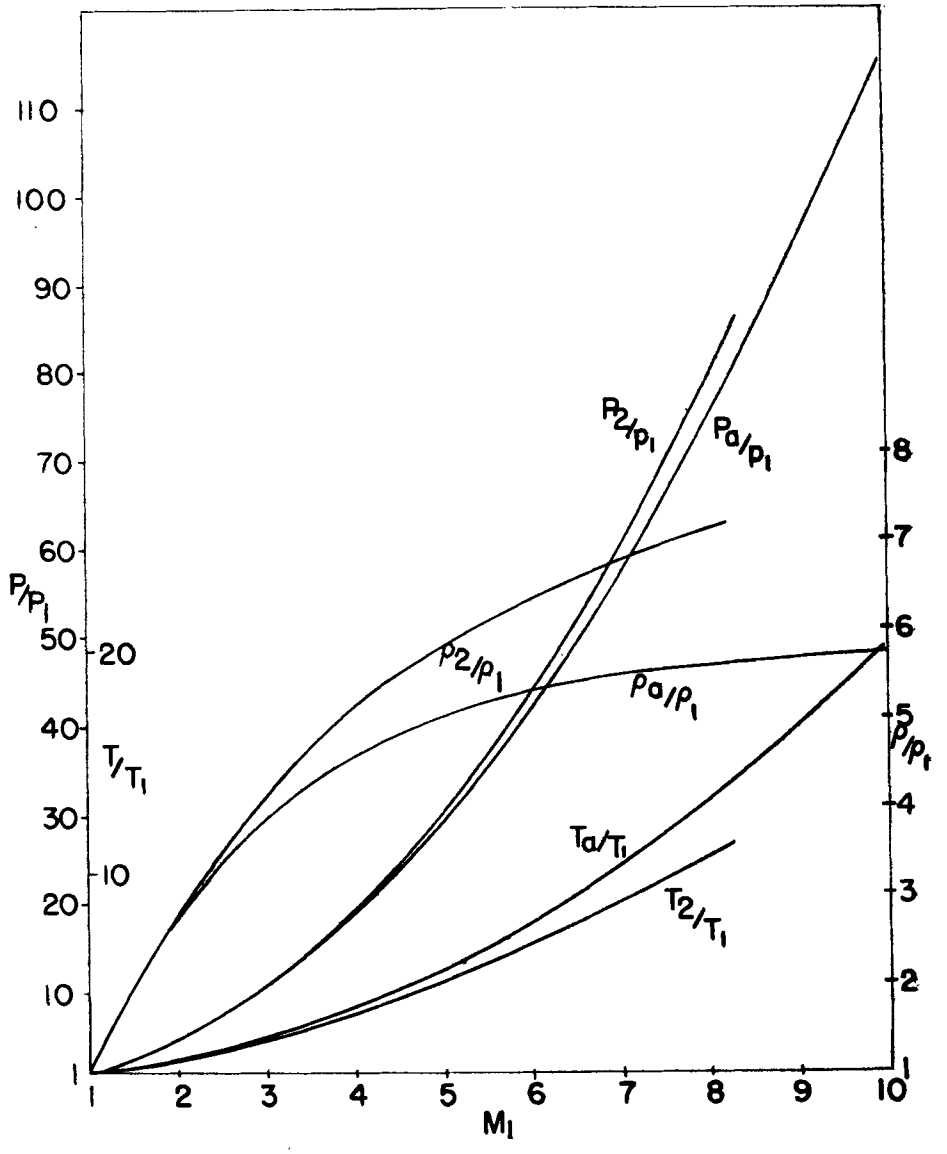

Figure 1. Density, pressure, and temperature ratios for shock waves in oxygen. The ratios with subscript a were calculated assuming constant C_p, while those with a subscript 2 are calculated by the Bethe–Teller method for variable Cp.

$T_1 = 296°$ K $\beta_1 = 3{\cdot}500$						
T_2° K	β_2	b	ρ_2/ρ_1	M_1	ρ_a/ρ_1	T_a° K
300	3·500	0·040	1·034	1·019	1·033	300
400	3·519	0·799	1·973	1·555	1·956	402
600	3·593	1·613	3·373	2·434	3·256	613
800	3·686	2·076	4·239	3·134	3·975	851
1000	3·775	2·387	4·834	3·720	4·408	1073
1200	3·853	2·613	5·273	4·245	4·698	1316
1400	3·921	2·787	5·612	4·717	4·899	1555
1600	3·981	2·926	5·883	5·148	5·049	1805
1800	4·034	3·041	6·108	5·563	5·159	2060
2000	4·082	3·138	6·300	5·948	5·253	2315
2200	4·126	3·223	6·457	6·314	5·330	2555
2400	4·168	3·298	6·615	6·663	5·393	2810
2600	4·208	3·366	6·749	6·999	5·444	3098

Table 1. Shock parameters for oxygen. Values of β were taken from the report by Woolley (1953 b).

Then, if y_n is the number of molecules in nth quantum state,

$$\frac{dy_n}{dt} = k_{n-1,n}\, y_{n-1} - k_{n,n-1}\, y_n + k_{n+1,n}\, y_{n+1} - k_{n,n+1} y_n. \tag{16}$$

By multiplying equation (16) by $nh\nu$, and summing over n, one can obtain the expression for the rate of change of E_{vib} with time:

$$\frac{\partial E_{\text{vib}}}{\partial t} = k_{10}\{1 - \exp(-h\nu/kT)\}\{E_{\text{vib}}(T) - E_{\text{vib}}\}, \tag{17}$$

where $E_{\text{vib}}(T)$ is the energy in vibration when the gas is in equilibrium with the external temperature T. If the external temperature does not change much during the process, the solution of equation (17) is given by

$$E_{\text{vib}} - E_{\text{vib}}(T) = C\exp(-t/\tau) \tag{18}$$

with

$$\frac{1}{\tau} = k_{10}\{1 - \exp(-h\nu/kT)\}. \tag{19}$$

For shock speeds of $M_1 = 7{\cdot}5$ in oxygen and $M_1 = 10$ in nitrogen, the assumption that T remains constant in the above integration may be in error by as much as 20%.

$T_1 = 296°$ K $\quad \beta_1 = 3{\cdot}497$						
$T_2°$ K	β_2	b	ρ_2/ρ_1	M_1	ρ_a/ρ_1	$T_a°$ K
300	3·497	0·040	1·041	1·024	1·041	300
400	3·500	0·782	1·938	1·547	1·938	401
600	3·521	1·542	3·237	2·397	3·211	604
1000	3·624	2·237	4·539	3·624	4·346	1074
1400	3·746	2·614	5·267	4·592	4·850	1495
1800	3·852	2·859	5·747	5·418	5·121	1980
2200	3·938	3·035	6·092	6·151	5·295	2460
2600	4·008	3·167	6·351	6·815	5·415	2960
3000	4·065	3·268	6·551	7·425	5·500	3450
3500	4·123	3·365	6·742	8·130	5·575	4080
4000	4·171	3·449	6·901	8·783	5·632	4690
4500	4·211	3·513	7·035	9·392	5·675	5330
5000	4·245	3·568	7·144	9·969	5·710	6010

Table 2. Shock parameters for nitrogen. Values of β were taken from the report by Woolley (1953 a).

Since the measurements that are carried out are actually on the density field behind the shock, it is necessary to find an expression connecting the change of density with the relaxation time.

If one assumes the transition region to be at a constant pressure, then the following relation between state a and the final state holds:

$$dE_{\text{vib}} = C_{\text{vib}}\, dT_{\text{vib}} = -C_p' dT. \tag{20}$$

For linear diatomic molecules, $C_p' = 7R/2$, and this may be considered as constant in the transition region, since translation and rotation are already fully excited. Equation (20) may then be integrated to give

$$E_{\text{vib}} - C_{\text{vib}} T_2 = -C_p' T + C_p' T_2,$$

so that

$$E_{\text{vib}} + C_p' T = C_{\text{vib}} T_2 + C_p' T_2 = C_p T_2. \tag{21}$$

Equations (17), (20), and (21) can then be combined and integrated to give

$$\frac{T-T_2}{T_a-T_2}=\exp(-C_p t/C_p'\tau). \tag{22}$$

From the perfect gas law, and the assumption that the pressure remains constant, this may be converted into an expression for the density change:

$$\frac{\rho-\rho_2}{\rho_a-\rho_2}=\frac{\rho_2}{\rho_a}\exp(-C_p t/C_p'\tau)\left[1+\frac{\rho_2-\rho_a}{\rho_a}\exp(-C_p t/C_p'\tau)\right]^{-1}. \tag{23}$$

The term $\frac{\rho_2-\rho_a}{\rho_a}\exp(-C_p t/C_p'\tau)$ in equation (23) is about 0·1, or less, for most of the experimental work reported here, so that to a first approximation, the whole term in square brackets may be set equal to 1. Therefore, not only the temperature, but also the density, approaches the final equilibrium value in an exponential manner.

The relaxation region is characterized by T_{vib} increasing from T_1 to T_2, and T_a decreasing to T_2. The energy in vibration E_{vib} also increases rapidly with time. The density and pressure both increase to the final equilibrium value with the same time constant as temperature. The change in pressure from state a to the final value, as shown by figure 1, is quite small and may be neglected in many calculations. However, the relatively large change in temperature and density is evident in the figures. It is this large change in density that makes the interferometer particularly suited to these measurements.

Landau & Teller have also developed a theory that helps to give a better understanding of the relatively slow exchange by collisions of vibrational energy in comparison with rotational energy. According to their work, the effectiveness of a given collision in exciting or de-exciting a periodic degree of freedom depends on the degree to which the collision can be considered as adiabatic. In this sense, a collision is assumed to be strictly adiabatic if the degree of freedom under consideration undergoes an infinite number of cycles during the time of contact. In such a case, there is zero probability that the mode will change its state during the collision. However, if the collision is not adiabatic, that is, if there is only a finite number of oscillations during the perturbing effect of the collision, then energy may be transferred from the translation to the degree of freedom being considered. To express this fact mathematically, they use the ratio

$$\chi=T_c/T_0, \tag{24}$$

where T_c is the duration of the collision, and T_0 the natural period of the degree of freedom. If χ is of the order of unity or less, then only a few collisions are necessary to bring the degree of freedom into equilibrium, while if χ is much larger than unity, many collisions will be needed for equilibrium. In their report, Bethe & Teller show that $\chi \leqslant 1$ for rotation, and therefore the rotational energy of a gas should come into equilibrium with the translatonal energy in just a few collisions. Experiments on the thickness of shocks in gases have shown this to be the case.

For a gas that has vibrational levels, this equilibrium between translation and rotation is not the final equilibrium state, since the vibrational energy will also change. When one considers vibration, T_c in equation (24) may be written

$$T_c \doteqdot r/\bar{v}', \tag{25}$$

where r is the range of strong molecular interaction, and $\bar{v}'$ is the relative velocity of the two colliding molecules. In equation (24), T_0 is simply the reciprocal of 2π times the frequency of vibration, so that

$$\chi \doteqdot \frac{2\pi\nu r}{\bar{v}'}. \tag{26}$$

For nitrogen at room temperatures this ratio is about 15. Since this is much larger than unity, it will take many hundreds of thousands of collisions to excite the vibrational states of nitrogen.

When $\chi \gg 1$, as is the case for vibration, Landau & Teller show that P_{10}, the probability per collision of de-exciting a molecule in the first excited state, is given by

$$P_{10} = C\exp(-\chi), \tag{27}$$

where C is a factor which depends on the geometry of the collision and is arbitrarily set equal to 1/10.

It may be noted from equations (26) and (27) that, as the temperature increases ($\bar{v}'$ increases), the probability of de-excitation per collision increases, which in turn shortens the relaxation time.

Now equation (27) must be generalized to include all of the molecules in the gas by averaging over the Maxwell velocity distribution. When this is done, it can be shown that one arrives at the following expression:

$$P_{10} = K_1 T^{-1/3}\exp(-K_2/T^{1/3}), \tag{28}$$

K_1 and K_2 are constants which depend on collision cross-sections and which cannot be accurately determined. Now P_{10} is related to k_{10} by the equation

$$NP_{10} = k_{10}, \tag{29}$$

where N is the number of collisions per unit time. Therefore,

$$\frac{1}{\tau} = NP_{10}\{1-\exp(-h\nu/kT)\}, \tag{30}$$

or since

$$N \propto pT^{-1/2},$$

$$\tau = K_1' T^{1/6}\exp(K_2/T^{1/3})/p\{1-\exp(-h\nu/kT\}. \tag{31}$$

For relatively low temperatures ($< 1000°$ K) equation (31) shows that $\log\tau \propto T^{-1/3}$, and this affords a convenient method of checking the theory. However, as the temperature rises, the factor $\{1-\exp(-h\nu/kT)\}$ can become important and must be taken into account in trying to compare experiment with theory if the accuracy of the experiments warrants it.

In recent years Schwartz & Herzfeld (1954) have elaborated on this theory, and have arrived at an equation which allows numerical computation of P_{10}. They give the result

$$\frac{1}{P_{10}} = \pi^2 \sqrt{\frac{3}{2\pi}} \left(\frac{h\nu}{\epsilon'}\right)^2 \left(\frac{kT}{\epsilon'}\right)^{1/6} \exp\left[\frac{3}{2}\left(\frac{\epsilon'}{kT}\right)^{1/3} - \frac{h\nu}{2kT} - \frac{\epsilon}{kT}\right], \qquad (32)$$

where ϵ and ϵ' are related to molecular constants.

Experimental equipment

In the course of normal operation, with helium at three atmospheres pressure in the high pressure chamber, and air at about 8 mm Hg pressure in the channel, experiments in the shock tube have been limited to $M_1 = 4$ in air. Experiments on vibrational relaxation times in CO_2, methane, and especially N_2O have been very successful with the present arrangement for two reasons. First, at the temperatures obtained behind shocks of this strength, there is sufficient vibrational excitation in these gases to cause a significant change in density from region *a* to the final equilibrium state in region 2. Second, the relaxation time is of such a value that the actual physical extension of the relaxing region behind the shock can be easily photographed and measured.

Measurements with the Mach–Zehnder interferometer on shock waves in nitrogen showed that the density ratio across the shock corresponded to ρ_a/ρ_1 instead of ρ_2/ρ_1. Hence, the vibrational adjustment has not taken place within the region of flow behind the shock that can be studied by this means. This was to be expected since it has been known for some time that relaxation times for diatomic gases are considerably longer than for polyatomic ones. An estimate of the lower limit of τ for nitrogen showed that $\tau > 200\,\mu$sec at 900° K for atmospheric pressure behind the shock. Since the relaxation time decreases as the temperature or pressure increases (according to equation (31)), it was necessary to devise a method of obtaining stronger shock waves. It was not practical to do this by simply reducing the pressure at the downstream end below 8 mm Hg, since the interferometer would have become increasingly insensitive.

After considering several possible methods for obtaining stronger shocks, it was decided to construct a converging channel which could be mounted inside the present tube. This plan permitted use of the interferometer, together with the associated optical equipment and many of the existing electronic triggering circuits and devices. The incident shock, of speeds up to $M_1 = 4$, was formed in the channel of the tube and allowed to converge through an area ratio of 34 : 1 to a channel of constant area.

The interferograms of the shock were taken after the wave had travelled about 20 inches along this final straight channel. Thus, if one assumes that the shock strength is constant in the straight section, then, for a density ratio of 6 across the shock, there should be over 3 inches of uniform flow behind the shock by the time it reaches the centre of the window. In practice, it was noticed that, as p_1 increased, irregularities in the flow

became more evident in the photographs. This is due to the increase in sensitivity of the interferometer as the density increases. However, in general, there were at least two inches of uniform flow behind the shock, and this distance was more than sufficient to measure relaxation times. The increase in shock strength was very considerable, and, for a wide range of initial pressure ratios across the diaphragm, the Mach number of the shock was almost doubled upon convergence. With helium as the driver gas, the upper limit for work in oxygen, nitrogen, and air was $M_1 = 7{\cdot}5$. For some of the work, hydrogen was used in the high pressure end in order to obtain shock strengths up to $M_1 = 10$ in nitrogen. At these shock strengths, relaxation effects were evident in both oxygen and nitrogen.

In order to check the Bethe–Teller method of calculation, two independent shock parameters had to be determined for each shock wave. The first of these measurements was the velocity of the shock, since from this velocity, and the speed of sound ahead of the shock, the Mach number can be determined. In order to measure the shock velocity, the time of passage of the shock past two points had to be determined. The detecting device that was used consists of a very narrow strip of evaporated gold whose resistance changed when it was heated up by the passage of a shock.* These gold films were of the order of 100 to 300 atoms thick, 1/2 mm wide, and 7 mm long. The resistance of the films was between 15 and 20 ohms, although films of widely varying resistance could be made to work. In use, a 22 volt battery and 2000 ohm resistance were set up in series with a film, then, when a shock passed over the film, a small change in voltage occurred across it. The rise time of this voltage pulse is determined only by the transit time of the shock across a film. As a test of this, a shock was allowed to travel lengthwise along a film one inch long, and the signal was put on an oscilloscope (see plate 2). The velocity of the shock, determined from the transit time of the shock along the film and the length of the film, agreed with the velocity measured by other means to within 1%. The narrow gold films that were used in the channel were oriented perpendicular to the motion of the shock, and the signal rise time was about $0{\cdot}5\ \mu$sec or less.

The gold films were made by evaporating a thin layer of gold directly on to sound recorder mending tape. This tape was chosen because it is the thinnest of the commercial adhesive tapes, with a thickness of about 2 mils. Strips of this tape could then be cut to the proper width and pressed in place gently, without harming the gold surface. The thickness of the films was estimated by weighing the filament both before and after the gold was evaporated and measuring the distance from the surface to the gold. From this information and the assumption that every atom of gold that strikes the surface sticks to it, a simple calculation gives the thickness of the film. It was found that the gold strips were extremely durable, showing no measurable change in resistance from shot to shot, and would last for dozens of shots if they were not scratched by a piece of the diaphragm. These strips of tape with the evaporated gold on the surface were stuck fast to

* The development of this technique was aided by information from R. J. Emrich, of Lehigh University, concerning a heat flux meter made of thin gold foil.

lucite plugs mounted flush with the surface of the upper wedge, as shown in plate 1. Contact from the film to the lead through screws was made by painting DuPont silver paint over the ends of the strip and the screw. This arrangement proved very satisfactory and enabled a broken film to be replaced with a minimum loss of time.

Provisions were made so that five of these thin films could be mounted along the upper wedge, although in most cases only two films were used. These were mounted five inches apart and situated so that v_1 was measured just before the photograph of the shock was taken.

The voltage output from the thin films amounted to 10 mv or more for the shock strengths used. This was more than 100 times the noise level of the apparatus. A typical oscilloscope trace of a thin film pulse is shown in plate 2. Since the signals were flat topped, they were differentiated before entering the chronograph. The timing traces on which the signals appeared had 5 μsec markers and the time of transit of the shock between the 2 films could be read to 0·2 μsec, giving an error in the time measurement of about $\pm 0{\cdot}4\%$ for $M_1 = 7$. The distance between the films was measured to within $\pm 0{\cdot}2\%$, so that the error in the Mach number determined in this manner is about $\pm 0{\cdot}6\%$ at $M_1 = 7$. As the Mach number decreases this error decreases, since the time measurement becomes increasingly accurate. For many shocks two separate measurements of the shock velocity were made, and these two measurements usually agreed very well.

The second measurement that was taken on each shock was the measurement of the density of the flow, which was made photographically with the use of the Mach–Zehnder interferometer. The illumination for the interferograms was obtained from a barium titanate spark with an effective duration of less than 0·3 μsec, which was sufficiently short to stop the motion of the shock. When charged to 10,000 volts, the illumination was intense enough for all purposes. The electrodes were made from stainless steel rods which were cleaned from time to time in order to keep the sparking reliable. The time at which the spark fired could be varied by an adjustable delay, the delay being triggered by the signal from one of the thin films.

From the interferograms the density in the region behind the shock can be determined from the fringe shift in the given region, as described by Bleakner, Weimer & Fletcher (1949). If δ is the shift of a fringe from its position at a given point in the field, and p_1 is the pressure ahead of the shock, then the density ρ at this point is given by

$$\frac{\rho}{\rho_1} = 1 + \frac{W}{p_1}\delta, \tag{33}$$

where W is a constant depending on the gas. The value of W can be either determined experimentally, by counting the fringe shift δ past a given point as the pressure in the shock tube is slowly changed and using the expression $W = \frac{p_2 - p_1}{\delta}$, or calculated from the equation

$$W = \frac{T p_s \lambda}{T_s l (n_s - 1)}, \tag{34}$$

where l is the width of the tube, n_s, T_s, and p_s are the index of refraction, temperature, and pressure of the gas at S.T.P., and λ is the wavelength of light used. Values of W obtained by these two methods differ by less than 0·5%.

Experimental results

Shock waves in argon, oxygen, nitrogen, and oxygen–nitrogen mixtures have been studied by the methods just described. Typical interferograms of shock waves in these gases, and the flow behind the shocks are shown in plates 3, 4, and 5. From these pictures and the simultaneous measurement of v_1, a check on the Bethe–Teller method of calculation has been carried out, and the vibrational relaxation times have been measured. The density ratios ρ_a/ρ_1 and ρ_2/ρ_1 were determined from the pictures and the use of equation (33) where δ_a is the fringe shift from in front of the shock to region a and δ_2 is the fringe shift to the equilibrium region. The fractional fringe shift can be measured, reproduceable to $\pm 0{\cdot}04$ fringes, by the use of an optical comparator. However, the determination of δ_a and δ_2 are not always this accurate. The value of δ_a depends on the point at which the fringe meets the shock. This measurement is greatly affected by the

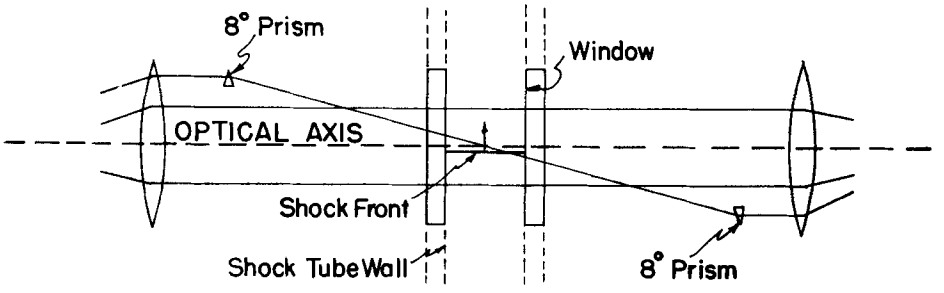

Figure 2. A schematic diagram of the offset prism technique which shows how the light is sent diagonally through the shock. The interferometer has been omitted.

apparent width of the shock in the interferogram (due to the spark duration and any slight angle the shock may have with the optical axis) and also by the rapid change of fringe position immediately behind the shock for short relaxation times. Thus the value of δ_a may be in error by as much as 0·2 fringes. The value of δ_2 for a gas showing relaxation may also be in error due to curvature of the undisturbed interferometer fringes. Since δ_2 must be measured 1 inch or more behind the shock in some cases, errors in δ_2 may be as high as 0·1 fringes. In general, errors in δ_a increase as the relaxation time decreases, and errors in δ_2 increase as the relaxation time increases.

In order to identify the integral number of the fringe shift across the shock, a technique using small angle offset prisms was used to send light obliquely through the shock.* A schematic diagram of the offset prism arrangement is shown in figure 2. This method of identifying the total fringe shift is a slight modification of a technique using an off-axis

* The offset prisms were first used in this laboratory by D. R. White.

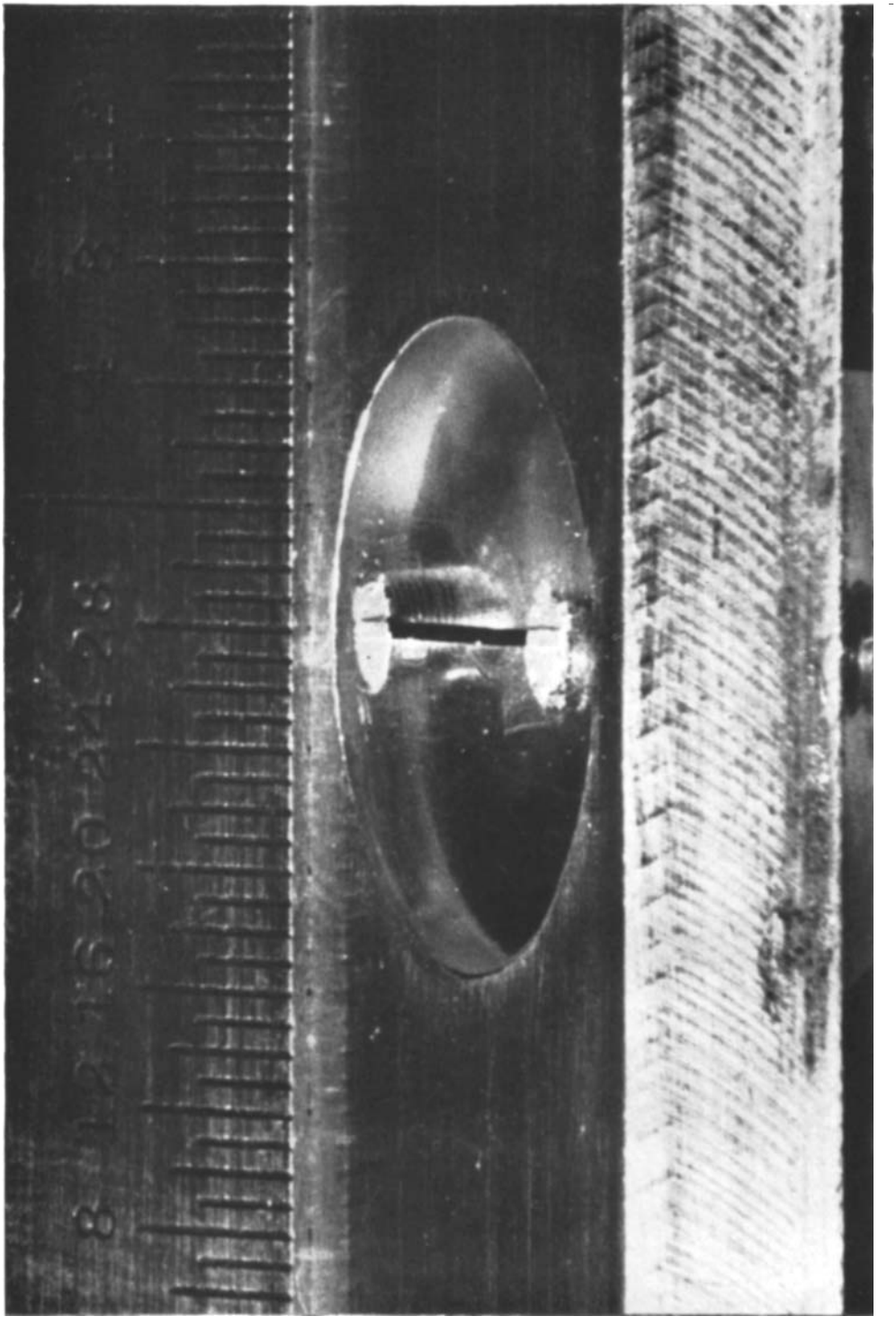

Plate 1. Close-up of a thin film mounted in the upper wedge. The smallest scale division on the ruler at the top is 1/32 of an inch.

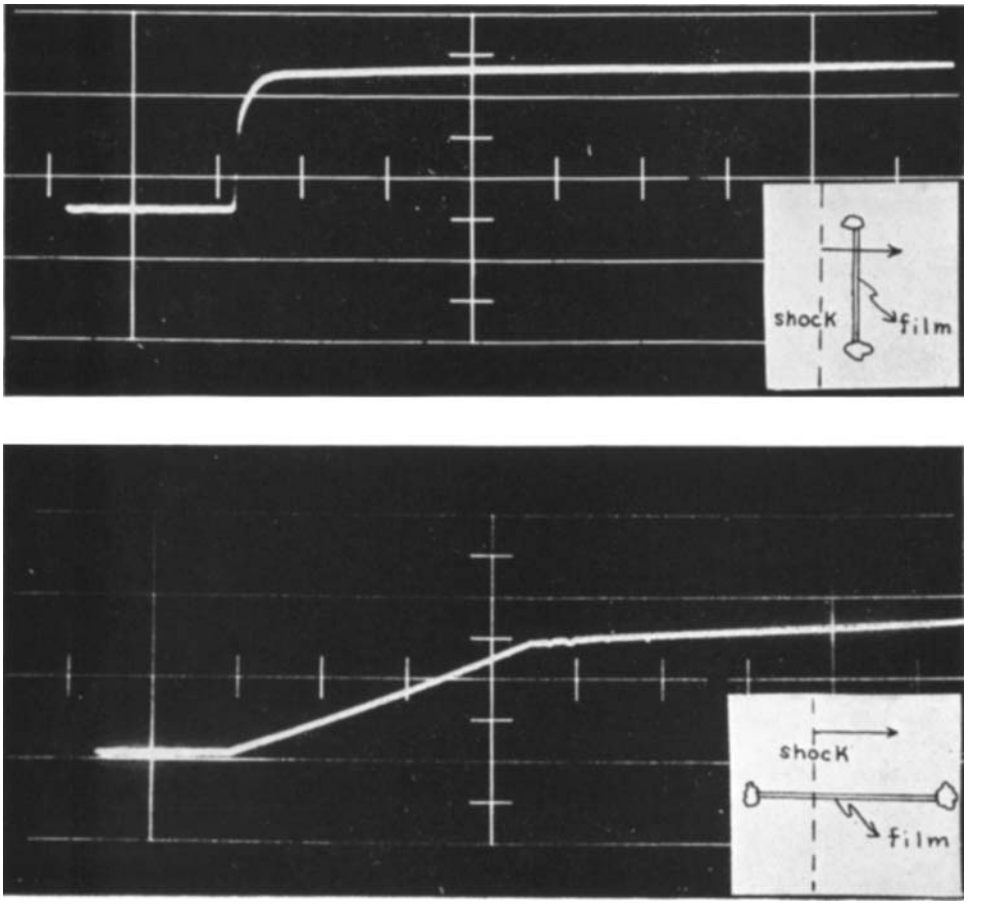

Plate 2. Typical voltage traces from the thin gold films. The sweep speed of the scope is 10 μ sec/cm.

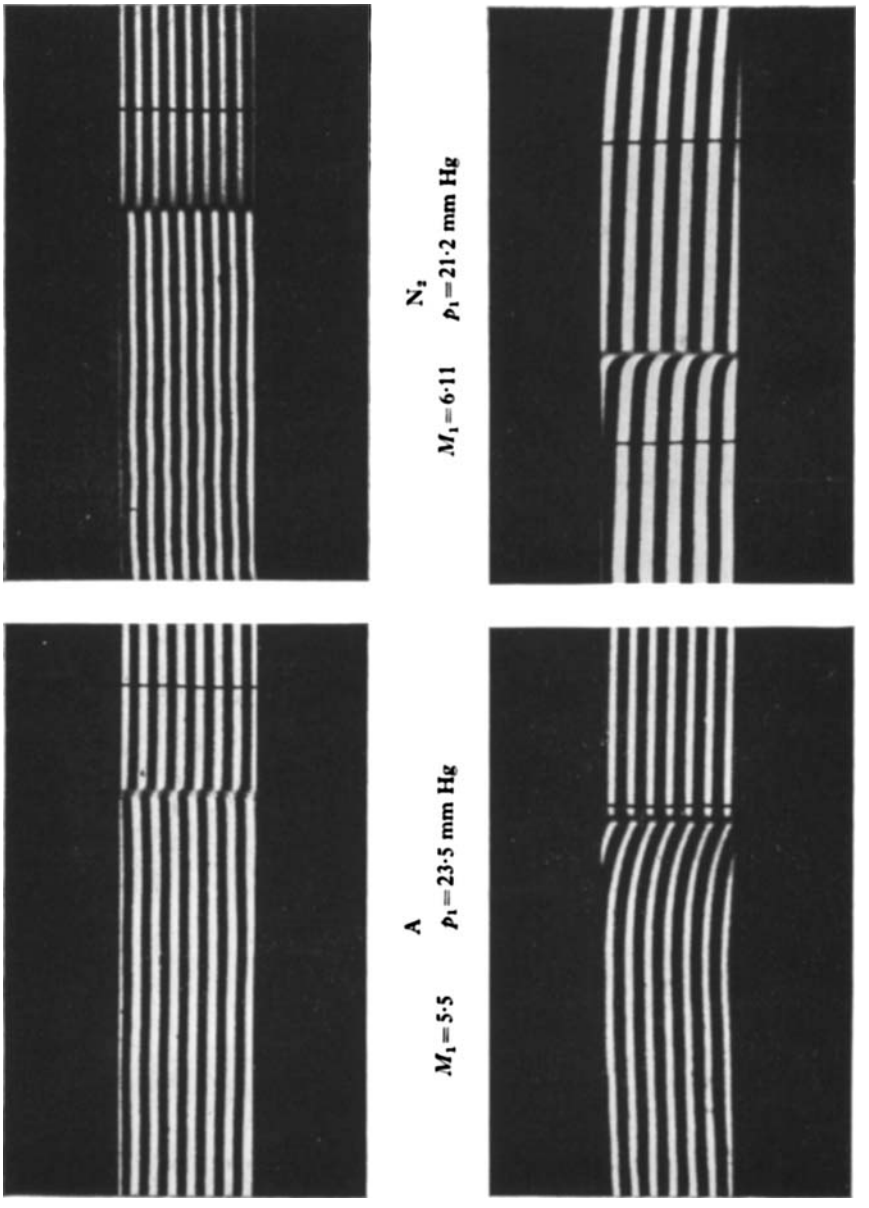

Plate 3. Shock waves in A, N_2 and O_2.

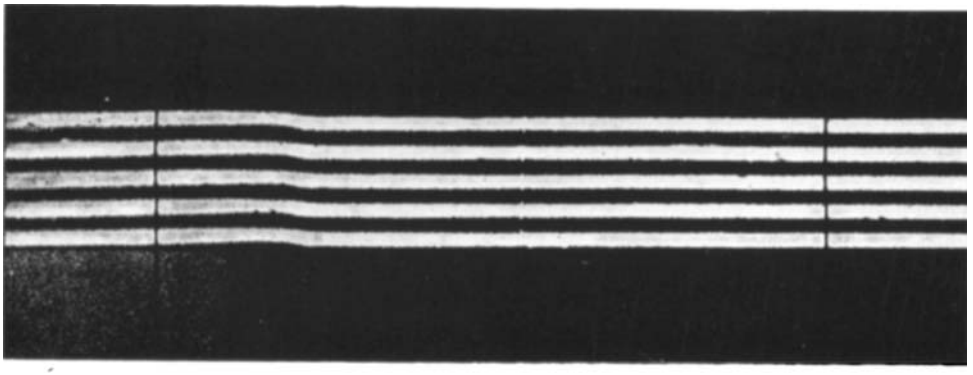

$M_1 = 10$ $\quad p_1 = 4$ mm Hg $\quad \tau = 4{\cdot}6$ μsec

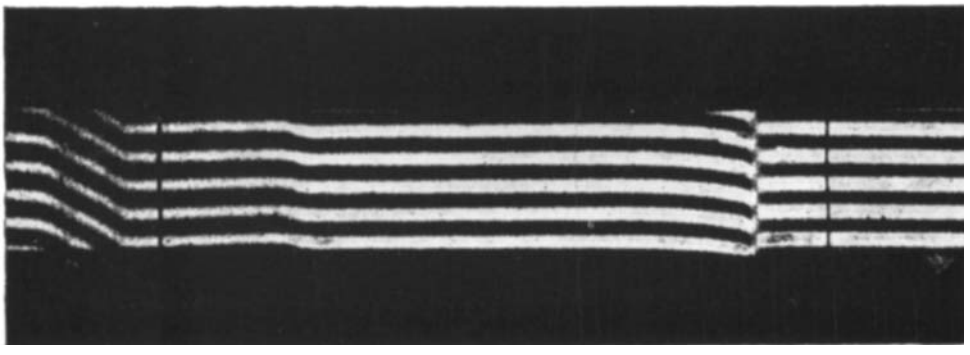

Plate 4. Disturbed and undisturbed interferograms showing total fringe shift and relaxation in N_2.

light source. Plate 4 shows an interferogram in which the shock can be seen in the channel and, at the same time, in the prism. It should be noted that a fringe can now be traced through the shock and the total fringe shift established.

As a check on the validity of the method of measuring M_1 and ρ/ρ_1, measurements were first made on a number of shocks in argon up to $M_1 = 8$. Since there is no excitation of any internal degrees of freedom ($\gamma = \text{constant}$) for these shock strengths, the values of ρ_2/ρ_1 as a function of M_1 can be calculated from the Rankine–Hugoniot equations with essentially no error. The measured values of ρ_2/ρ_1 and M_1 were compared with the calculated values, and the agreement proved satisfactory. A shock wave passing through argon is shown in plate 3. It can be seen that the fringes do not shift in the region behind the shock, indicating that the density is constant.

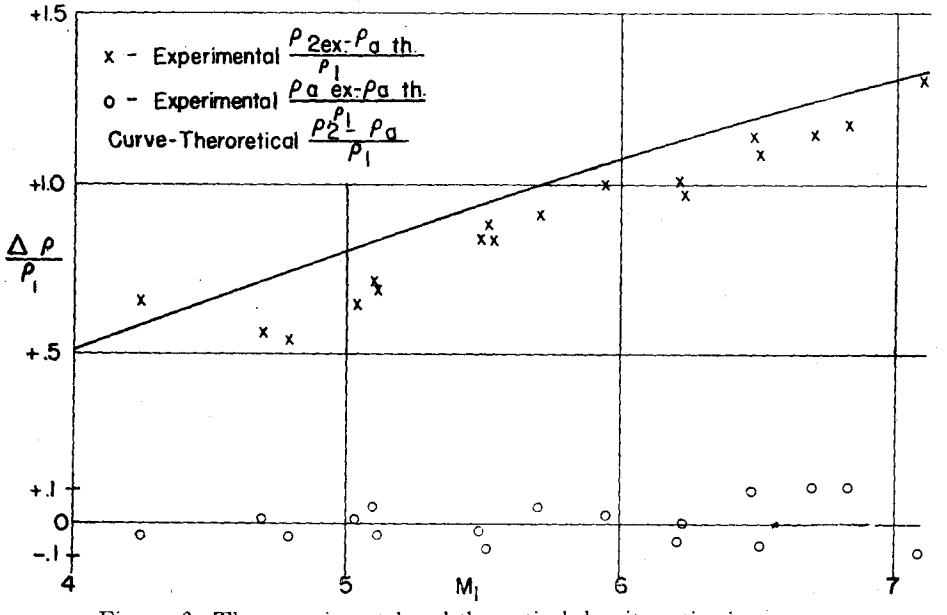

Figure 3. The experimental and theoretical density ratios in oxygen.

A comparison of the two interferograms of shocks in oxygen with the one in argon (plate 3) shows a considerable difference in the region behind the shock. In oxygen, the fringes shift from the value at the shock to a higher final value in the equilibrium region. This shift in fringes reflects the density change in the transition region from state *a* to the final equilibrium state. From the interferograms the values of ρ_a/ρ_1 and ρ_2/ρ_1 have been determined for a number of shock waves in oxygen.

Values of $\Delta\rho/\rho_1$ where, $\Delta\rho$ is the difference between the experimental and theoretical values of ρ_a for the one case, and the difference between the experimental value of ρ_2 and the theoretical value of ρ_a for the other case, are plotted against the experimentally determined Mach number in figure 3. The difference between the theoretical values of ρ_2/ρ_1 and ρ_a/ρ_1 has been

plotted for comparison. It can be seen from the figure that the experimental values of ρ_a/ρ_1 agree very well with the theoretical calculation. However, the results also show that the measured values of ρ_2/ρ_1 lie consistently below the calculated values by about 1 to 2%. Since there is only one vibrational mode in oxygen, and since any dissociation effects would tend to make the density higher instead of lower, this discrepancy in ρ_2/ρ_1 is believed to be due to impurities and errors in measurement. The purity of the oxygen was not very high, and, for the strongest shocks, there was about 5% of nitrogen present in the gas ahead of the shock. As the value of p_1 increased, this percentage of nitrogen decreased. It is difficult to obtain a tube of oxygen of high purity with the present arrangement, since the pumping system takes the pressure down to only about 0·5 mm Hg, and the oxygen cannot be flushed through the shock tube like argon or nitrogen, since it would react with the pump oil. Hence, the purity of the oxygen varied between 95% and 99% for the work reported here, with the main impurity being nitrogen. The nitrogen still has essentially no energy in vibration by the time the density ratio reaches ρ_2/ρ_1, so that the role of nitrogen as an impurity should be to cause the density in the region after the oxygen relaxes to be lower than the calculated value. Therefore, this may explain part of the discrepancy, but it is believed that another error was present in the determination of the pressure which may have been as large as 1% for some cases.

The relaxation time in oxygen has also been determined from the interferograms. Equations (23) and (33) can be combined to give an expression relating the fringe shift in the transition region to the relaxation time. Thus,

$$\frac{\delta-\delta_2}{\delta_a-\delta_2}=\frac{\rho_2}{\rho_a}\exp(-C_p t/C_p'\tau)\left[1+\frac{\rho_2-\rho_a}{\rho_a}\exp(-C_p t/{}'_p C\tau)\right]^{-1}. \tag{35}$$

Since the denominator is nearly equal to 1, by taking the natural logarithm one obtains the result

$$\log\delta \doteqdot -C_p t/C_p'\tau+K \tag{36}$$

or, since $t=x/\bar{v}$, where x is the distance behind the shock and $\bar{v}$ is the average velocity of flow behind the shock,

$$\tau=\frac{C_p}{C_p'}\frac{(x_b-x_a)}{\bar{v}\log(\delta_a/\delta_b)}. \tag{37}$$

This equation may now be used to calculate τ from the interferograms. Figure 4 shows some experimental plots of $\log\delta$ versus the distance behind the shock front. The fact that these points lie approximately on a straight line justifies the replacement of the term in square brackets in (35) by unity. These plots give one confidence in this method of measuring τ. The values of (x_b-x_a) and $\log(\delta_a/\delta_b)$ are determined from plots such as these, and $\bar{v}$ is taken as the arithmetical average of v_a and v_2.

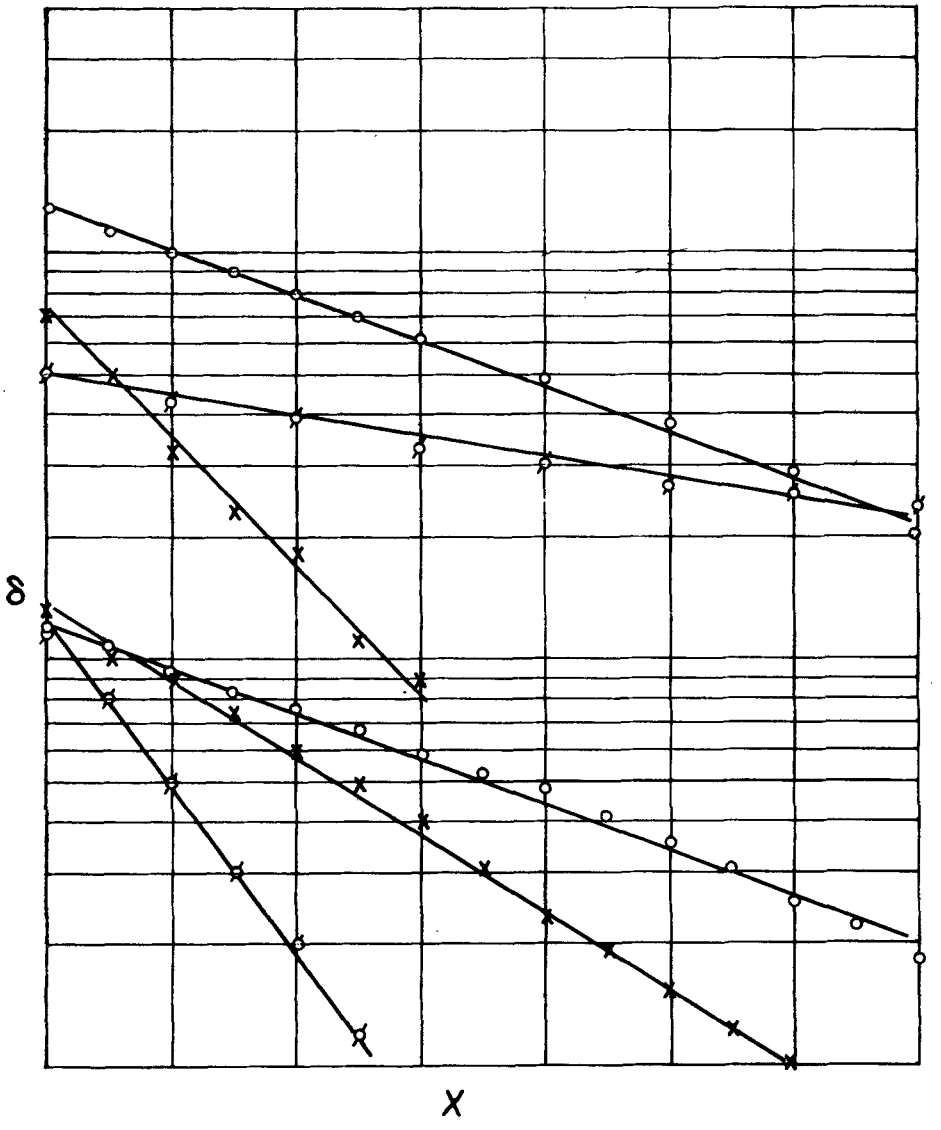

Figure 4. Typical plots of fringe shift versus distance behind the shock. δ and x are in arbitrary units.

The values of τ for oxygen using this method have been calculated for a number of shock strengths and the logarithm of the results has been plotted against $\overline{T}^{-1/3}$ in figure 5. To the extent that the factor $\{1-\exp(-h\nu/kT)\}$ in equation (31) can be neglected, this sort of plot gives a direct check on the validity of the Landau–Teller theory. The relaxation time calculated from equation (37) is τ at the pressure p_2, so that these

values must then be corrected to atmospheric pressure for the plot in figure 1. The temperature $\bar{T}$, which is used for this graph is the average of T_a and T_2. It can be seen from the figure that the experimental points appear to lie on a slightly curved line instead of a straight line.

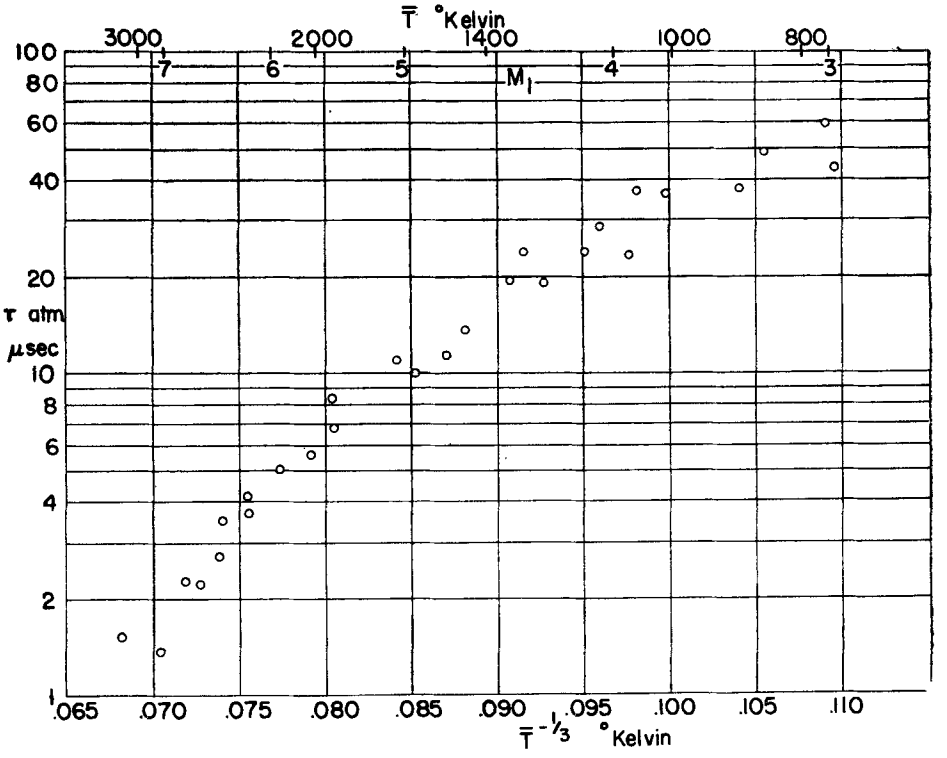

Figure 5. Vibrational relaxation times for atmospheric pressure in oxygen.

The oxygen, and also the other gases, were dried in a 4-foot long drying system containing $CaSO_4$. Since the percentage of water vapour decreases as the pressure of the gas in the drier increases, the gas was flowed through this pipe at 20 to 30 p.s.i. However, with the large quantity of gas to be handled in the shock tube, it is difficult to obtain the same purity as one can in a small volume. For the experiments in oxygen, the amount of water vapour varied from about 1 part in 4000 for $M_1 = 7$, $p_1 = 10$ mm Hg, to about 1 part in 20,000 for $M_1 = 4{\cdot}25$, $p_1 = 50$ mm Hg. Since it is known that water vapour is very effective in bringing about vibrational equilibrium in many gases, it was believed that, for the stronger shocks, the greater amount of water vapour was lowering the relaxation time. However, data on the relaxation times in the air, in which the gas was not dried, seem to show that, for strong shocks, water vapour in these concentrations does not shorten τ by a measurable amount. Later experiments also showed that nitrogen did not have a large effect in reducing the relaxation time of the oxygen, so that the effect of impurities on τ is believed to be very small.

Results of measurements of ρ_a/ρ_1 in the range of $M_1 = 5$–10 for N_2 are plotted in figure 6. For the pictures in which relaxation was evident, ρ_2/ρ_1 was measured, and these values are also plotted in figure 6. As in figure 3, the values actually plotted are $\Delta\rho/\rho_1$, where $\Delta\rho$ is the difference in ρ, as explained before. The agreement between theory and experiment is within the experimental limits for these values. It can be seen that, for the stronger shocks and smaller p_1, the accuracy of the experiments decreases.

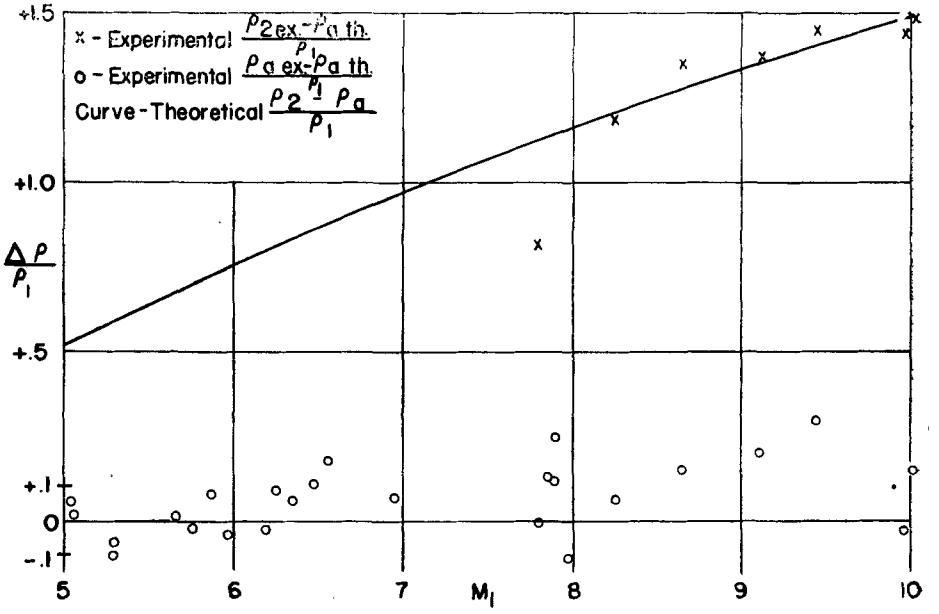

Figure 6. The experimental and theoretical density ratios in nitrogen.

The purity of the nitrogen used in these experiments was considerably greater than the purity of the oxygen. The shock tube was pumped out to 0·5 mm Hg pressure and then nitrogen which had been dried by the $CaSO_4$ drier was flushed though the tube for about three minutes before the final value of p_1 was set. This technique should keep the presence of water vapour in the experiments to less than 1 part in 10^5.

Relaxation times in nitrogen have also been calculated from pictures such as in plate 4 by the method outlined above. The results of these measurements are shown in figure 7, in which $\log\tau$ is again plotted against $T^{-1/3}$, as an experimental check on the Landau–Teller theory. From the few points plotted, it appears that the data check the theory within the accuracy of the measurements.

Figure 8 shows a much wider range of τ and T, and includes relaxation times from shock tube measurements in oxygen, nitrogen, and CO_2, Pitot tube measurements in nitrogen, and sound dispersion measurements for oxygen (Kneser & Knudsen 1935, and Knötzel & Knötzel 1948).

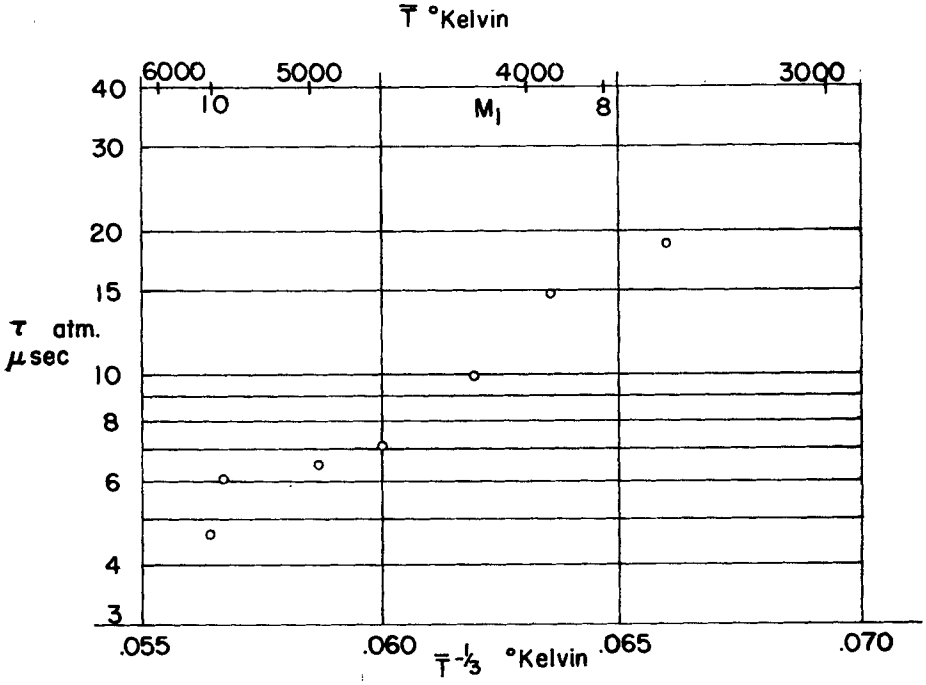

Figure 7. Vibrational relaxation times for atmospheric pressure in nitrogen.

From the relaxation times, which are directly calculated from the experimental data, one can also obtain transition probabilities. In the theoretical work by Herzfeld & Schwartz (1954) on oxygen and nitrogen, theoretical values of P_{10} for temperatures up to 3000° K are reported. Consequently, for the purpose of comparison, it is convenient to express the results in terms of P_{10} as well as τ.

From equation (30),

$$\frac{1}{\tau} = NP_{10}\{1-\exp(-h\nu/kT)\}.$$

But

$$N = \mathcal{N} q\bar{v}', \tag{38}$$

where $\mathcal{N}$ is the number of molecules per unit volume, q is the collision cross-section, and $\bar{v}'$, the mean relative velocity of the molecules, is

$$\bar{v}' = \sqrt{\left(\frac{8}{\pi}\frac{kT}{m}\right)}. \tag{39}$$

Now values of collision cross-sections are not well known and depend greatly on the type of molecular model that is used. It is also known that the value changes with temperature, decreasing to approximately a constant value as the temperature increases. Therefore, it will be assumed here that, in the temperature range under consideration, the value of q is constant. Values of N as a function of temperature were calculated assuming that, for

collisions between oxygen molecules, $q = 3{\cdot}6 \times 10^{-15}\,\mathrm{cm}^2$, and, for collisions between nitrogen molecules, $q = 4{\cdot}1 \times 10^{-15}\,\mathrm{cm}^2$. From these values of N and the average experimental values of τ, P_{10} was calculated for a number of temperatures. These values are tabulated along with those of Herzfeld & Schwartz in table 3. Values of P_{10} from the Kantrowitz & Huber (1947) measurements on nitrogen, and those of Knötzel & Knötzel (1948) in oxygen, are also included in the table. The agreement is really excellent considering previous attempts to calculate relaxation times.

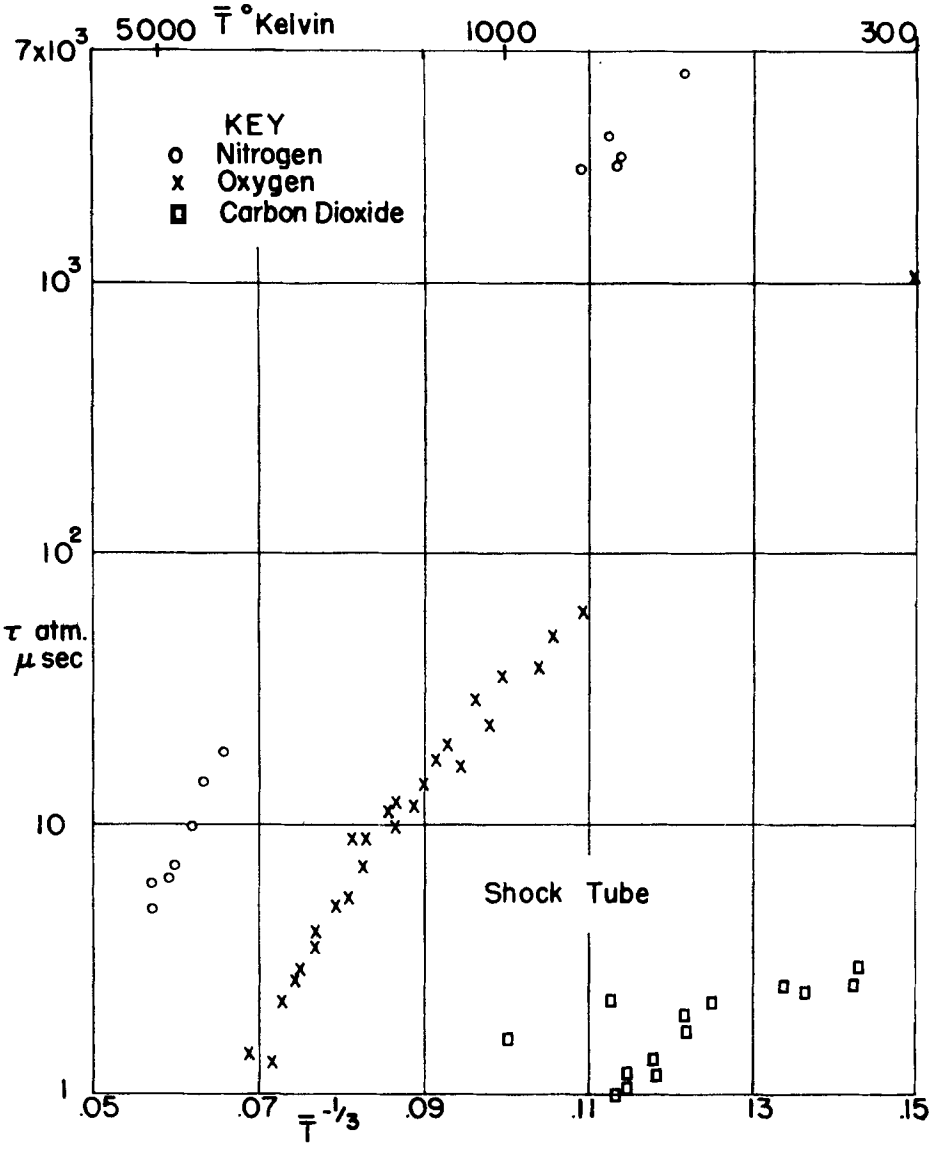

Figure 8. Relaxation times in N_2, O_2, and CO_2.

$T°$ K	P_{10} exptl.	P_{10} calc.
Oxygen $q=3{\cdot}6\times10^{-15}$ cm^2		
288	4×10^{-8}	1×10^{-8}
900	$1{\cdot}1\times10^{-5}$	3×10^{-6}
1200	$2{\cdot}4\times10^{-5}$	$1{\cdot}3\times10^{-5}$
1800	$9{\cdot}8\times10^{-5}$	$8{\cdot}6\times10^{-5}$
2400	$3{\cdot}7\times10^{-4}$	$5{\cdot}5\times10^{-4}$
3000	$1{\cdot}2\times10^{-3}$	$1{\cdot}5\times10^{-3}$
Nitrogen $q=4{\cdot}1\times10^{-15}$ cm^2		
600	3×10^{-8}	17×10^{-10}
1800		$1{\cdot}1\times10^{-6}$
3000	$3{\cdot}1\times10^{-5}$	$1{\cdot}6\times10^{-5}$
4000	$9{\cdot}7\times10^{-5}$	
5000	$2{\cdot}5\times10^{-4}$	

Table 3. Experimental and theoretical values of P_{10}. q is the gas-kinetic collision cross-section. The experimental values for oxygen are due to Knötzel & Knötzel (1948) ; those for nitrogen are due to Kantrowitz & Huber (1947). The calculated values are taken from Herzfeld & Schwartz (1954).

Investigations were also conducted on oxygen–nitrogen mixtures, and the effect of N_2-O_2 collisions on the approach to equilibrium for O_2 was determined for a narrow range of temperature. The oxygen and nitrogen for these experiments were mixed in a tank outside the shock tube and allowed to stand for several hours. By this means, it is believed that the gases were adequately mixed before being used in the tube. Values of ρ_2/ρ_1 for these mixtures for the intermediate state have been calculated by the Bethe–Teller method. It is assumed that, in this intermediate state, the energy in the vibrational states of nitrogen had not had time to change, so that the value of $\beta_2(N_2)$ is still 3·50, which is the value appropriate to 300°K. The value of β for the mixture is then given by

$$\beta=\sum_i p_i\beta_i, \tag{40}$$

where p_i and β_i are the partial pressure and energy content of the ith component. The values of ρ_2/ρ_1 for this intermediate state have been measured for four different mixtures of oxygen and nitrogen including air. These experimental values, together with the theoretical curves, are plotted in figure 9. Values of ρ_a/ρ_1 have also been measured for these mixtures and are included in the figure. The numbers plotted here are the actual values of ρ/ρ_1 instead of the changes in this quantity.

The relaxation times of the oxygen in the mixtures have been calculated for a number of pictures like those in plate 5. As a first approximation, these relaxation times were reduced to atmospheric relaxation times by assuming that O_2-N_2 collisions were not effective in bringing about equilibrium

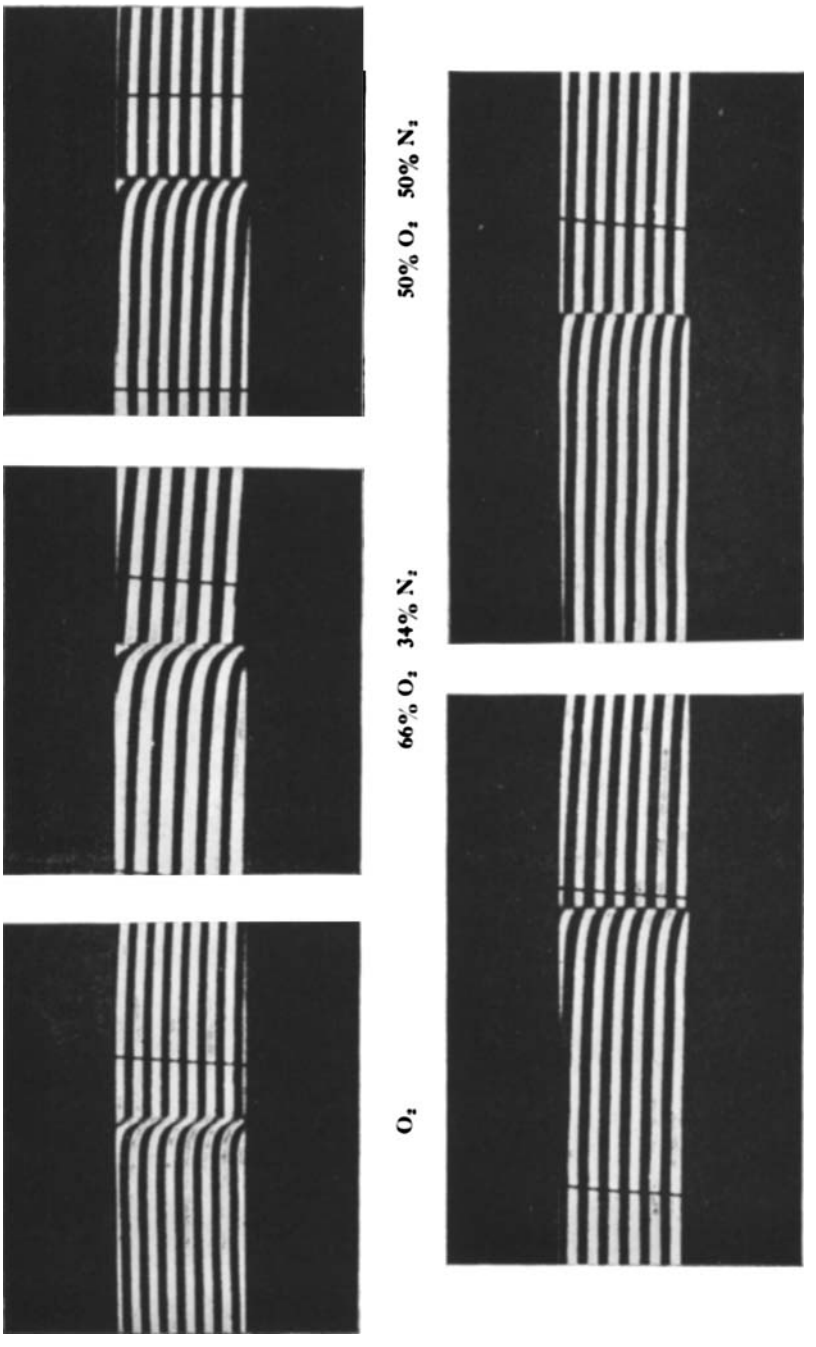

Plate 5. Vibrational relaxation in oxygen-nitrogen mixtures. $M_1 \doteqdot 6, p_1 = 21$ mm Hg for all cases.

in the oxygen. Thus, it was assumed that the relaxation was taking place at a pressure equal to the partial pressure of the oxygen. The value of τ, corrected for this pressure, is too low, which means that the relaxation takes place at a higher effective pressure. Now, if one assumes that $O_2 - N_2$ collisions are 40% as efficient as $O_2 - O_2$ collisions in bringing about equilibrium in the oxygen, then the relaxation time, as shown by the experimental

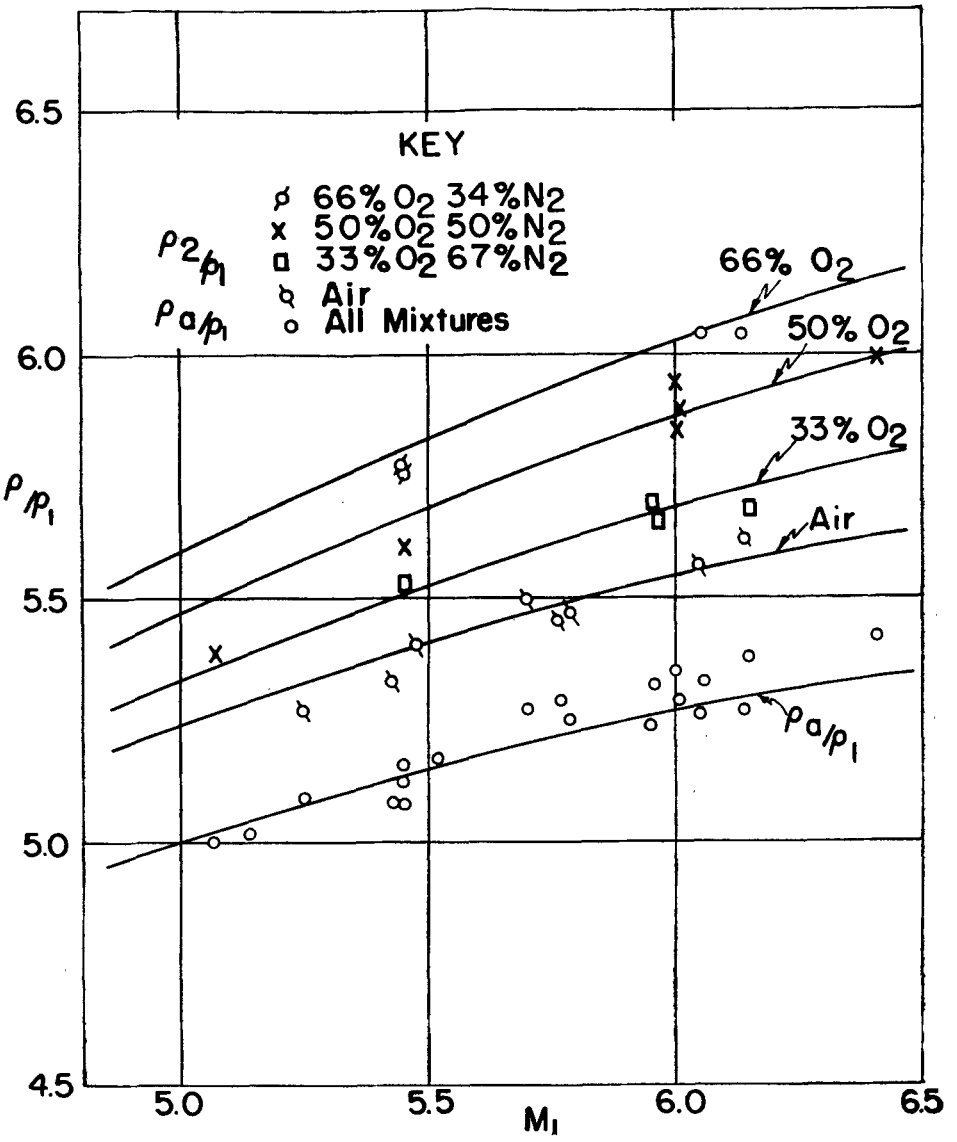

Figure 9. The density ratios in O_2—N_2 mixtures.

points in figure 10, is in good agreement with the average curve for oxygen. For higher efficiencies for $O_2 - N_2$ collisions, the value of τ becomes correspondingly higher. Therefore, for this range of temperature at least, $O_2 - N_2$ collisions are only about 40% as effective in transferring a quantum

of energy to the oxygen as O_2-O_2 collisions. Previous estimates have placed the effectiveness of O_2-N_2 collisions at about 5 times that of O_2-O_2 collisions.

Most of the experiments were carried out on dried gases. However, some experiments were conducted in undried air to see if the effect of water vapour could be detected. The relaxation times for 3 different shock strengths in undried air are also included in figure 10, and it may be

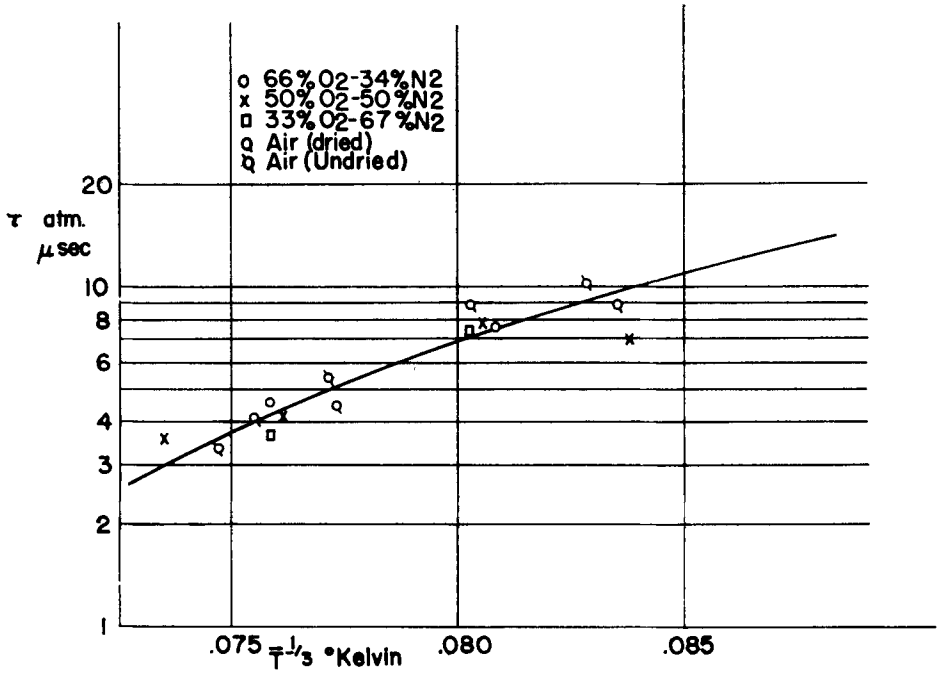

Figure 10. Relaxation times in O_2-N_2 mixtures for atmospheric pressure assuming O_2-N_2 collisions are only 40% as effective in transferring energy as O_2-O_2 collisions The curve is the average value of τ for pure O_2.

seen that the water vapour did not have a measurable effect on τ. The amount of water vapour in these shots was estimated to be 1 to 3 parts in a thousand. It is known that the effectiveness of impurities in bringing about equilibrium decreases as the temperature increases, and it is believed that this is the reason the nitrogen and water vapour had a smaller effect on the oxygen than anticipated. For example, if an O_2-H_2O collision is only 50 to 100 times as effective as an O_2-O_2 collision, this would not affect τ enough to be detected in these experiments.

I would like to express my appreciation to Professor Griffith and Professor Bleakney for their help and advice. My associates at the shock wave laboratory, and especially Mr Wesley Smith, provided much assistance in carrying out the experiments. The research was supported by the Office of Naval Research.

References

BETHE, H. E. & TELLER, E. 1951 Deviations from thermal equilibrium in shock waves. Issued by Engineering Research Institute, University of Michigan.

BLEAKNEY, W., WEIMER, D. K. & FLETCHER, C. H. 1949 *Rev. Scien. Inst.* **20,** 807.

GRIFFITH, W. 1950 *J. Appl. Phys.* **10,** 1319.

GRIFFITH, W., BRICKL, D. & BLACKMAN, V. (to be published).

HERZFELD, K. F. & RICE, F. O. 1928 *Phys. Rev.* **31,** 691.

HERZFELD, K. F. 1953 Relaxation phenomena in gases, *Thermodynamics and Physics of Matter,* Princeton University Press.

KANTROWITZ, A. 1942 *J. Chem. Phys.* **10,** 145.

KANTROWITZ, A. & HUBER, P. W. 1947 *J. Chem. Phys,* **15,** 275.

KNESER, H. O. & KNUDSEN, V. O. 1935 *Ann. der Phys,* **21,** 682.

KNÖTZEL, H. & KNÖTZEL, L. 1948 *Ann. der Phys,* **2,** 393.

LANDAU, L. & TELLER, E. 1936 *Phys. Z. Sowiet,* **10,** 34.

PIERCE, G. W. 1925 *Proc. Acad. Sci. Amst.* **60,** 271.

RESLER, E. L., LIN, S. C. & KANTROWITZ, A. 1950 *J. Appl. Phys.* **23,** 1390.

SCHWARTZ, R. N. & HERZFELD, K. F. 1954 *J. Chem. Phys.* **22,** 767.

SMILEY. E., WINKLER, E. & SLAWSKY, Z. 1954 *J. Chem. Phys.* **22,** 2018.

WOOLLEY, H. W., 1953 a Thermodynamic properties of gaseous nitrogen, *Nat. Bur. Stan., Rep.* no. 2287.

WOOLLEY, H. W. 1953 b Thermodynamic properties of molecular oxygen, *Nat. Bur. Stan., Rep.* no 2611.